Chemical Dynamics of the Formation of the 1,3-Butadiynyl Radical ($C_4H(X^2\Sigma^+)$) and Its Isotopomers

Xibin Gu,[†] Ying Guo,[†] Alexander M. Mebel,[‡] and Ralf I. Kaiser*[,†]

Department of Chemistry, University of Hawaii at Manoa, Honolulu, Hawaii 96822, and Department of Chemistry and Biochemistry, Florida International University, Miami, Florida 33199

Received: May 26, 2006; In Final Form: July 27, 2006

The reaction of dicarbon molecules in their electronic ground, $C_2(X^1\Sigma_g^+)$, and first excited state, $C_2(a^3\Pi_u)$, with acetylene, $C_2H_2(X^1\Sigma_g^+)$, to synthesize the 1,3-butadiynyl radical, $C_4H(X^2\Sigma^+)$, plus a hydrogen atom was investigated at six different collision energies between 10.6 and 47.5 kJ mol^{-1} under single collision conditions. These studies were contemplated by crossed molecular beam experiments of dicarbon with three acetylene isotopomers $C_2D_2(X^1\Sigma_g^+)$, C_2HD $(X^1\Sigma^+)$, and $^{13}C_2H_2(X^1\Sigma_g^+)$ to elucidate the role of intersystem crossing (ISC) and of the symmetry of the reaction intermediate(s) on the center-of-mass functions. On the singlet surface, dicarbon was found to react with acetylene through an indirect reaction mechanism involving a diacetylene intermediate. The latter fragmented via a loose exit transition state via an emission of a hydrogen atom to form the 1,3-butadiynyl radical $C_4H(X^2\Sigma^+)$. The $D_{\infty h}$ symmetry of the decomposing diacetylene intermediate results in collision-energy invariant, isotropic (flat) center-of-mass angular distributions of this microchannel. Isotopic substitution experiments suggested that at least at a collision energy of 29 kJ mol^{-1}, the diacetylene isotopomers are long-lived with respect to their rotational periods. On the triplet surface, the reaction involved three feasible addition complexes located in shallower potential energy wells as compared to singlet diacetylene. The involvement of the triplet surface accounted for the asymmetry of the center-of-mass angular distributions. The detection of the 1,3-butadiynyl radical, $C_4H(X^2\Sigma^+)$, in the crossed beam reaction of dicarbon molecules with acetylene presents compelling evidence that the 1,3-butadiynyl radical can be formed via bimolecular reactions involving carbon clusters in extreme environments such as circumstellar envelopes of dying carbon stars and combustion flames.

1. Introduction

The linear 1,3-butadiynyl radical in its $^2\Sigma^+$ electronic ground state holds the global minimum among six C_4H isomers (Figure 1).[1] In recent years, this hydrogen-deficient molecule has received considerable attention due to its potential importance as a precursor to polycyclic aromatic hydrocarbons (PAHs) and possibly to fullerenes[2] in the interstellar medium,[3−6] in hydrocarbon-rich atmospheres of planets and their moons,[7,8] and in combustion processes.[9−11] The butadiynyl radical was first detected in 1975 in low-temperature argon and neon matrixes in its electronic ground state.[12] These studies were supplemented by Thaddeus et al.[13] and Cernicharo et al.[14] recording millimeter wave spectra of the 1,3-butadiynyl radical.[15,16] The spectroscopic data also assisted an identification of the butadiynyl radical in extreme environments such as in the circumstellar envelope of the dying carbon star IRC+10216 (CW Leo)[17,18] and in cold molecular clouds such as TMC-1.

Despite the importance of the 1,3-butadiynyl radical in combustion processes and in astrochemistry as a potential precursor to form polycyclic aromatic hydrocarbon (PAH) molecules, the question "How is the 1,3-butadiynyl radical actually synthesized in these environments?" is far from being resolved.[19] In cold molecular clouds such as in TMC-1, chemical reaction models suggest that this radical is formed via a dissociative recombination of an electron from the cosmic radiation field with a diacetylene cation. However, these models underestimate the observed column densities by up to 1 order of magnitude.[20] This indicates that important formation pathways to the 1,3-butadiynyl radical have not been incorporated into

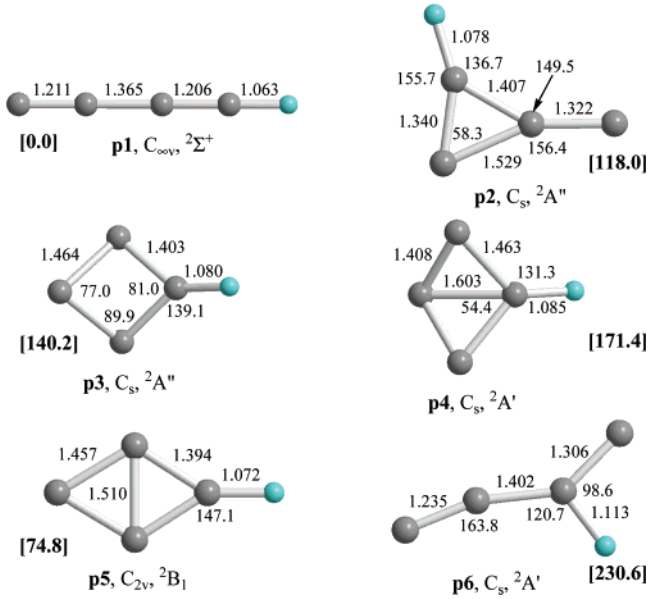

Figure 1. Structures of six C_4H isomers p1−p6 together with their point groups and electronic ground states. The relative energies with respect to the most stable 1,3-butadiynyl radical (p1) are given in square brackets in units of kJ mol^{-1}. Bond lengths are given in angstroms, bond angles in degrees.

[†] University of Hawaii at Manoa.
[‡] Florida International University.

10.1021/jp063256l CCC: $33.50
Published on Web 09/14/2006

these models yet. An early crossed beam study of dicarbon molecules with acetylene at collision energy of 24.1 kJ mol^{-1} suggested an alternative formation route.[21] Here, 1,3-butadiynyl, $C_4H(X^2\Sigma^+)$, radicals were found to be synthesized under single collision conditions via a neutral−neutral reaction through dicarbon versus hydrogen exchange pathways on the singlet and triplet surfaces via indirect scattering dynamics.

However, various facets of this reaction have remained unanswered so far. First, the detailed dynamics and importance of the singlet versus triplet surface in the synthesis of the 1,3-butadiynyl molecule have not been fully resolved yet. Second, the previous investigation could not discriminate whether the forward−backward symmetric angular distribution originating from the decomposition of a diacetylene intermediate (HCCCCH, $X^1\Sigma_g^+$) was the result of a long-lived complex or the consequence of a "symmetric" intermediate ($D_{\infty h}$). In this context, a "symmetric intermediate" is defined as a decomposing complex in which a leaving hydrogen atom can be interconverted by a 2-fold rotation axis. This would give an equal probability that the hydrogen atom is leaving in a direction of θ or $\pi - \theta$; as a result, the center-of-mass angular distribution is forward−backward symmetric although the lifetime of the intermediate might be less than its rotation period.[22] This behavior has been observed in the $C(^3P_j) + C_2H_2(X^1\Sigma_g^+)$ reaction.[22] Here, a C_2 symmetric triplet propargylene intermediate (HCCCH(X^3B)) was found to produce an isotropic center-of-mass angular distribution at collision energies between 8.8 and 45.0 kJ mol^{-1}. Third, it is important to investigate potential effects of intersystem crossings from the triplet to the singlet surface and vice versa. Last, the limited signal-to-noise ratio achieved in the previous study hindered an explicit conclusion if the molecular hydrogen elimination channel was open or not.

To answer these open questions, we expanded the previous study and investigated the collision-energy dependent chemical dynamics of the reaction between dicarbon molecules in their $X^1\Sigma_g^+$ and $a^3\Pi_u$ electronic states with acetylene, $C_2H_2(X^1\Sigma_g^+)$, at six collision energies between 10.6 and 47.5 kJ mol^{-1}. The collision-energy dependent changes in the shape of the center-of-mass angular distributions are expected to yield valuable information on the involvement of the singlet versus triplet surface. In addition, we carried out the reaction with isotopically labeled $^{13}C_2H_2(X^1\Sigma_g^+)$ and $C_2HD(X^1\Sigma^+)$ at a selected collision energy of 29 kJ mol^{-1} to reduce the symmetry of the singlet diacetylene intermediate from $D_{\infty h}$ to $C_{\infty v}$; this is expected to help elucidate to what extent the forward−backward symmetric center-of-mass angular distribution of the microchannel originating from the singlet surface is the effect of the symmetry of the singlet diacetylene intermediate or truly from a long-lived complex behavior. Third, reactions with $C_2D_2(X^1\Sigma_g^+)$ were conducted to compare the derived center-of-mass functions with those obtained for $C_2H_2(X^1\Sigma_g^+)$; this is expected to enable us to comment on the role of intersystem crossing; the latter should be facilitated by the incorporation of two deuterium atoms. Finally, we carried out additional experimental investigations at enhanced signal-to-noise ratios on the molecular hydrogen loss pathway.

2. Experimental Setup and Data Processing

The experiments were conducted under single collision conditions in a crossed molecular beams machine at The University of Hawaii.[23] Briefly, the main chamber consists of a 2300 L stainless steel box and is evacuated to the low 10^{-8} Torr region. Both source chambers are placed inside the main chamber so that the reactant beams cross perpendicularly. Pulsed dicarbon beams were produced in the primary source by laser ablation of graphite at 266 nm by focusing 4−10 mJ per pulse at 30 Hz on the rotating carbon rod.[24] The ablated species were seeded in neat carrier gas (helium, neon, or argon, 99.9999%, 3040 Torr, Table 1) released by a Proch−Trickl pulsed valve. After passing a skimmer, a four-slot chopper wheel mounted after the ablation zone selected a part out of the seeded dicarbon beam, which crossed then a pulsed acetylene beam (C_2H_2; 99.99% after removal of the acetone stabilizer via a zeolitic trap and acetone-dry ice cold bath) under a well-defined collision energy in the interaction region (Table 1). At a selected collision energy of 29 kJ mol^{-1}, the acetylene beam was replaced by beams of isotopically labeled $^{13}C_2H_2(X^1\Sigma_g^+)$, C_2HD ($X^1\Sigma^+$), and $C_2D_2(X^1\Sigma_g^+)$ (Cambridge Isotopes; 99.8−99.9%). At all velocities, the ablation beams contain dicarbon in its $X^1\Sigma_g^+$ electronic ground state as well as in its first electronically excited $a^3\Pi_u$ state; at the present stage, the concentration of the singlet versus triplet states are unknown.[24] Although the primary beam contains carbon atoms and tricarbon molecules as well, these species were found not to interfere with the reactive scattering signal of the dicarbon−acetylene reaction at mass-to-charge ratios (m/z) of 49 (C_4H^+) and 48 (C_4^+). Here, tricarbon reacts with acetylene only at collision energies larger than about 85 kJ mol^{-1};[25] signal from the reaction of atomic carbon with acetylene only shows up at m/z values of 37 (C_3H^+) and lower.[26] The reactively scattered species are monitored using a triply differentially pumped quadrupole mass spectrometric detector (QMS) in the time-of-flight (TOF) mode after electron-impact ionization of the neutral molecules at 200 eV electron energy. Our detector can be rotated within the plane defined by the primary and the secondary reactant beams to allow taking angular resolved TOF spectra. By taking and integrating the TOF spectra, we obtain the laboratory angular distribution, i.e., the integrated signal intensity of an ion of distinct m/z versus the laboratory angle. For each angle, we accumulated up to 1.5 $\times$ 10^6 TOF spectra. The velocity of the supersonic dicarbon beam was monitored frequently after taking the data for five angles. Reference angles were chosen at the corresponding center-of-mass angles to calibrate fluctuating dicarbon beam intensities.

TABLE 1: Peak Velocities (v_p), Speed Ratios (S) and Center-of-Mass Angles (Θ_{CM}) Together with the Nominal Collision Energies of the Dicarbon and the Acetylene reactants (E_c)

beam	v_p (ms^{-1})	S	E_c, kJ mol^{-1}	Θ_{CM}
$C_2(X^1\Sigma_g^+/a^3\Pi_u)$/Ar	944 ± 8	5.0 ± 0.1	10.6 ± 0.1	46.0 ± 0.3
$C_2(X^1\Sigma_g^+/a^3\Pi_u)$/Ne	1060 ± 17	4.7 ± 0.5	12.1 ± 0.2	42.7 ± 0.5
$C_2(X^1\Sigma_g^+/a^3\Pi_u)$/He	1629 ± 6	5.2 ± 0.1	21.6 ± 0.2	31.0 ± 0.2
$C_2(X^1\Sigma_g^+/a^3\Pi_u)$/He	1956 ± 23	5.7 ± 0.2	29.0 ± 0.5	26.5 ± 0.2
$C_2(X^1\Sigma_g^+/a^3\Pi_u)$/He	2362 ± 42	4.9 ± 0.3	39.9 ± 0.2	22.5 ± 0.4
$C_2(X^1\Sigma_g^+/a^3\Pi_u)$/He	2608 ± 36	4.1 ± 0.2	47.5 ± 1.2	20.5 ± 0.2
$C_2H_2(X^1\Sigma_g^+)$	902 ± 2	16.0 ± 1.0		
$C_2D_2(X^1\Sigma_g^+)$	896 ± 5	16.0 ± 1.0		
$^{13}C_2H_2(X^1\Sigma_g^+)$	895 ± 5	16.0 ± 1.0		
$C_2HD(X^1\Sigma^+)$	898 ± 4	16.0 ± 1.0		

Information on the chemical dynamics were obtained by fitting these TOF spectra of the reactively scattered products and the product angular distribution in the laboratory frame (LAB) using a forward-convolution routine that is described in detail in refs 27 and 28. This procedure initially assumes an angular distribution $T(\theta)$ and a translational energy distribution $P(E_T)$ in the center-of-mass reference frame (CM). TOF spectra and the laboratory angular distribution were then calculated from these $T(\theta)$ and $P(E_T)$ taking into account the beam spreads and the apparatus functions. Best fits of the TOF and laboratory angular distributions were achieved by refining the $T(\theta)$

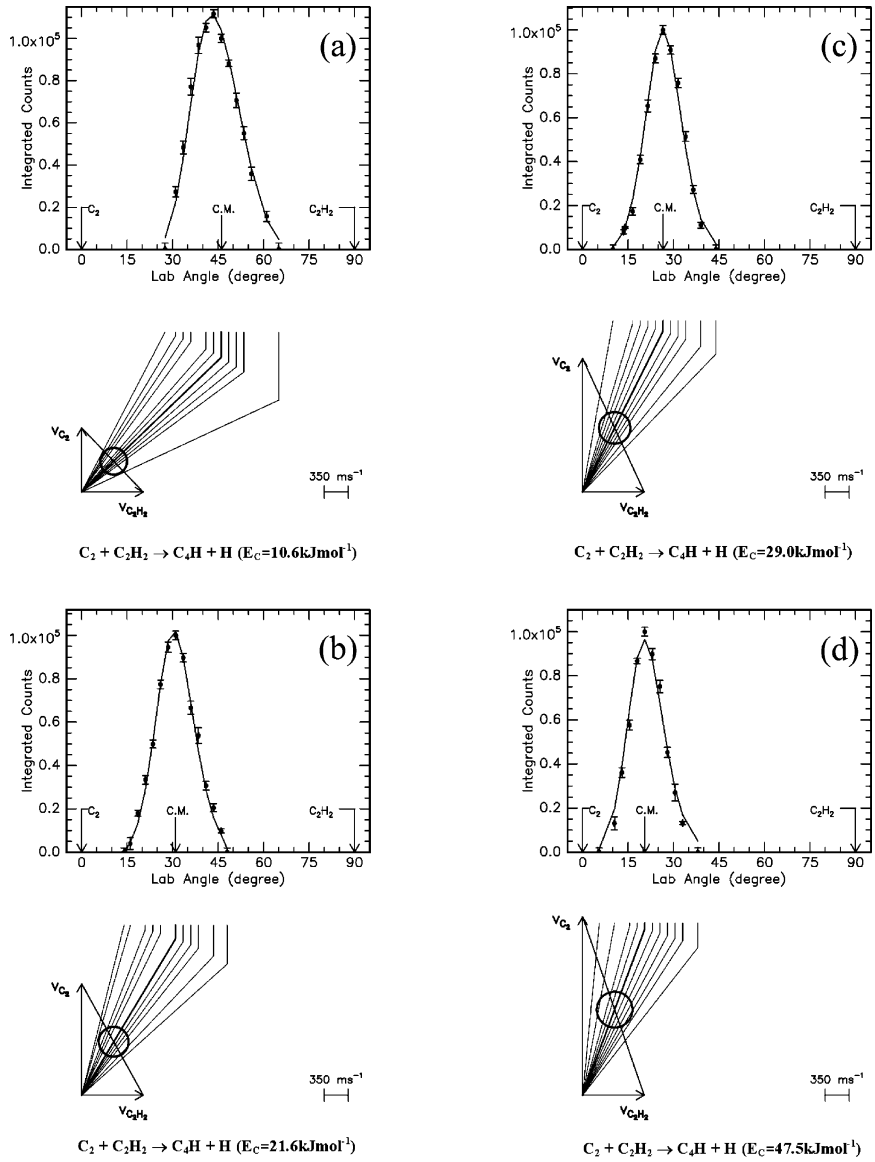

Figure 2. Newton diagrams for the reaction of $C_2(X^1\Sigma_g^+/a^3\Pi_u) + C_2H_2(X^1\Sigma_g^+) \rightarrow C_4H(X^2\Sigma^+) + H(^2S_{1/2})$. The inner and outer circles stand for the maximum center-of-mass recoil velocities of the 1,3-butadiynyl product for the dicarbon reactant in its $X^1\Sigma_g^+$ and $a^3\Pi_u$ electronic states, respectively. Also shown are the laboratory angular distribution of the 1,3-butadiynyl product channel at $m/z = 49$. Circles and 1σ error bars indicate experimental data, the solid lines the calculated distributions. CM designates the center-of-mass angle. Newton diagrams and laboratory angular distributions are shown for four selected nominal collision energies of 10.6 (a), 21.6 (b), 29.0 (c), and 47.5 kJ mol^{-1} (d). The corresponding time-of-flight (TOF) spectra are shown in Figure 3.

parameters and the points of the $P(E_T)$. The final outcome is the generation of a product flux contour map. This presents the differential cross section, $I(\theta,u) \sim P(u) \times T(\theta)$, of the product that reports the intensity of the heavy reaction product as a function of angle θ and product center-of-mass velocity u. This map serves as an image of the reaction and contains all the information of the reactive scattering process.

3. Electronic Structure Calculations

The details of the potential energy surfaces for the dicarbon ($C_2(X^1\Sigma_g^+)/C_2(a^3\Pi_u)$) versus atomic hydrogen replacement were described in our previous publication.[21] Here, we present new results on the hitherto unexplored molecular hydrogen elimination from the intermediates in the singlet and triplet states to produce tetracarbon C_4 in its electronic ground ($X^3\Sigma_g^-$) and/or first excited states ($a^1\Sigma_g^+$). Second, we investigated direct abstraction pathways of a hydrogen atom by a dicarbon molecule to form the ethynyl radical ($C_2H(X^2\Sigma^+)$). Geometries of various intermediates, transition states, and products involved have been optimized using the hybrid density functional B3LYP/6-311G-(d,p) level of theory.[29] Vibrational frequencies have been computed using the same theoretical method; relative energies have been refined by single-point restricted coupled cluster RCCSD(T)/6-311+G(3df,2p) calculations.[30] The ab initio GAUSSIAN 98[31] and MOLPRO 2002[32] program packages were utilized.

4. Results

4.1. Laboratory Data. *4.1.1. C_2/C_2H_2 System.* We observed signal at mass-to-charge ratios of $m/z = 49$ (C_4H^+), 48 (C_4^+), 37 (C_3H^+), and 36 (C_3^+). At all laboratory angles, the TOF spectra at $m/z = 49$ (C_4H^+) (Figures 2 and 3) and 48 (C_4^+) are, after scaling, superimposable. This indicates that the molecular hydrogen elimination channel is absent; the signal at $m/z = 48$ originated solely from a dissociative ionization of the C_4H parent in the ionizer; upper limits of the molecular hydrogen loss

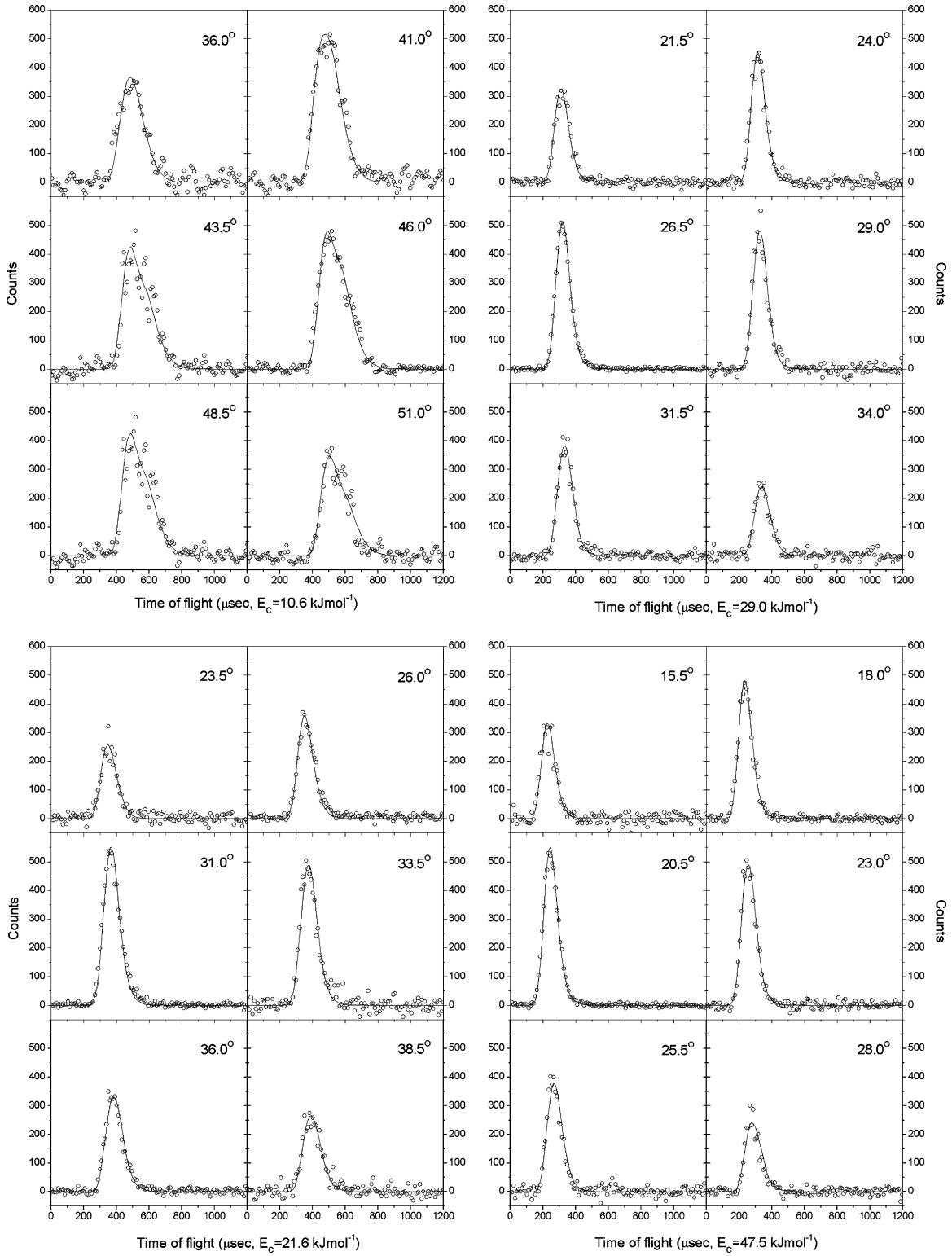

Figure 3. Time-of-flight data at $m/z = 49$ for various laboratory angles at selected collision energies of 10.6 (upper left), 21.6 (upper right), 29.0 (lower left), and 47.5 kJ mol^{-1} (lower right). Open circles represent experimental data; the solid line represents the fit. TOF spectra have been normalized to the relative intensity at each angle.

pathway can be given to less than 1%. Depending on the collision energy and the inherent recoil spheres of the tricarbon hydride product of the carbon plus acetylene reaction, signal at $m/z = 37$ (C_3H^+) either depicted identical patterns (a fit was achieved with identical center-of-mass functions compared to the TOFs recorded at $m/z = 49$ (C_4H^+)) or had to be fit with two contributions, one from the dissociative ionization of the C_4H parent in the ionizer and a second from the tricarbon hydride radical product of the carbon−acetylene reaction. TOFs taken at $m/z = 36$ differ strongly from the higher masses. Here, the signal arises from fragmentation of the C_4H (dicarbon−acetylene reaction product) and C_3H parents (carbon−acetylene reaction product) in the ionizer to C_3^+ (slow parts) and from the $C_3(X^1\Sigma_g^+) + H_2(X^1\Sigma_g^+)$ channel (fast part) which is open in the reaction of atomic carbon, $C(^3P_j)$ with acetylene.[25]

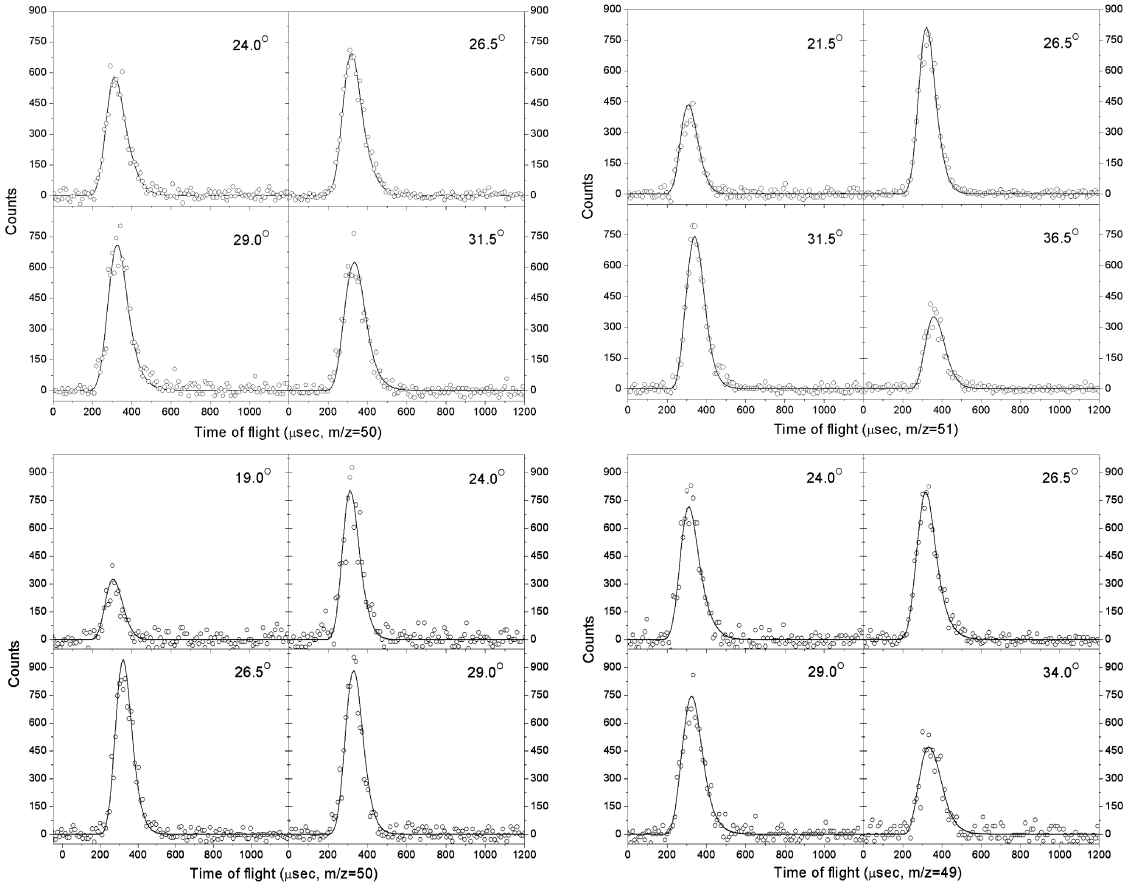

Figure 4. Time-of-flight data for various laboratory angles recorded in the crossed beams reactions of dicarbon molecules with $C_2D_2(X^1\Sigma_g^+)$ ($m/z = 50$; C_4D^+; upper left), $^{13}C_2H_2(X^1\Sigma_g^+)$ ($m/z = 51$; $^{13}C_2C_2H^+$; upper right), and $C_2HD(X^1\Sigma^+)$ ($m/z = 50$; C_4D^+; lower left) ($m/z = 49$; C_4H^+; lower right) at a nominal collision energy of 29 kJ mol^{-1}. Open circles represent experimental data; the solid line represents the fit. TOF spectra have been normalized to the relative intensity at each angle.

The most probable Newton diagrams of the reactions of dicarbon $C_2(X^1\Sigma_g^+/a^3\Pi_u)$ with acetylene to form 1,3-butadiynyl ($C_4H(X^2\Sigma^+)$) plus atomic hydrogen ($H(^2S_{1/2})$) and the laboratory angular distributions of the C_4H product recorded at $m/z = 49$ are displayed in Figure 2 at selected collision energies. The corresponding TOF spectra are presented in Figure 3. The LAB distributions are relatively narrow and spread only over 32° in the scattering plane. As expected from the kinematics of the reaction, the angular spread of the scattering signal increases by about 10−42° from the highest to the lowest collision energy of 10.6 ± 0.1 kJ mol^{-1}. The relatively small angular spreads suggest that a comparatively small fraction of the total available energy is released as translational energy of the 1,3-butadiynyl and atomic hydrogen products. This is also reflected in the relatively small width of the TOF spectra of only 250−350 μs.

4.1.2. C_2/C_2D_2, C_2/C_2HD, and $C_2/^{13}C_2H_2$ Systems. Considering the C_2D_2 and $^{13}C_2H_2$ reactants, we recorded TOF spectra at mass-to-charge ratios of $m/z = 50$ (C_4D^+) and $m/z = 51$ ($^{13}C_2C_2H^+$), respectively, at a collision energy of 29 kJ mol^{-1}. In case of acetylene-d_1 (C_2HD), the atomic hydrogen and deuterium loss pathway was monitored at $m/z = 50$ (C_4D^+) and $m/z = 49$ (C_4H^+). Figures 4 and 5 summarize the TOF spectra for the atomic hydrogen/deuterium loss channels and derived the laboratory angular distributions, respectively. We also investigated if the deuterium versus hydrogen and ^{13}C versus ^{12}C labeling in the acetylene reactant could open up the molecular hydrogen elimination channel. We examined the D_2, HD, and H_2 emission pathways for the acetylene-d_2, acetylene-d_1, and acetylene-$^{13}C_2$ reactants at mass-to-charge ratio of $m/z = 48$ (C_4^+) and $m/z = 50$ ($^{13}C_2C_2^+$). However, signals of all TOF spectra were found to originate, similarly to the dicarbon plus acetylene system, from dissociative fragmentation of the corresponding isotopomers of the C_4H radical.

4.2. Center-of-Mass Functions. Figure 6 presents the translational energy distributions in the center-of-mass-frame, $P(E_T)$, together with the center-of-mass angular distributions, $T(\theta)$; the corresponding flux contour maps are compiled in Figure 7. In case of the dicarbon−acetylene reactions, best fits of the TOF spectra and the LAB distributions were achieved at each collision energy with a single $P(E_T)$ extending to a maximum translational energy, E_{max}, of 47 kJ mol^{-1} ($E_c = 10.6$ kJ mol^{-1}), 50 kJ mol^{-1} ($E_c = 12.1$ kJ mol^{-1}), 60 kJ mol^{-1} ($E_c = 21.6$ kJ mol^{-1}), 70 kJ mol^{-1} ($E_c = 29.0$ kJ mol^{-1}), 80 kJ mol^{-1} ($E_c = 39.9$ kJ mol^{-1}), and 90 kJ mol^{-1} ($E_c = 47.5$ kJ mol^{-1}). Due to the kinematics of the reaction, i.e., an emission of a light hydrogen atom, the fits are relatively insensitive to the high energy cutoff: adding or cutting the high energy tail by ±5 kJ mol^{-1} did not influence the quality of the fit. Because the maximum translational energy presents simply the sum of the collision energy and the absolute of the exoergicity of the reaction, the magnitude of E_{max} can be utilized to compute the reaction exoergicity. Averaging over six collision energies, we determine that the C_4H plus atomic hydrogen channel is exoergic by 39.9 ± 5.0 kJ mol^{-1}. Also, all $P(E_T)$s depict a flat and very broad plateau between 3 and 17 kJ mol^{-1}; the latter presents an upper limit at the highest collision energy investigated in this study. These data may suggest that at least one reaction channel exhibits an exit barrier and, hence, a significant geometry as well as electron density change from the fragmenting C_4H_2 intermediate to the products resulting in a repulsive

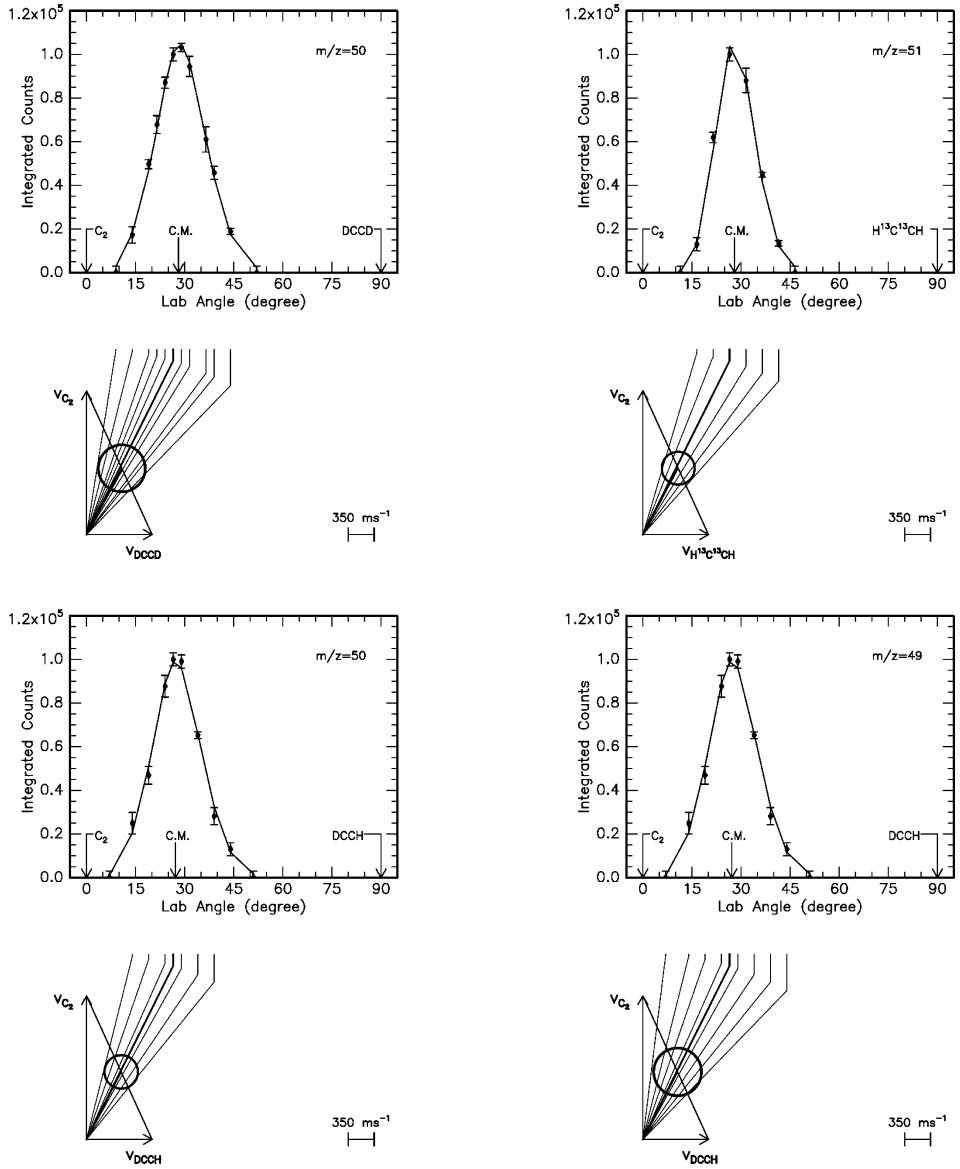

Figure 5. Newton diagrams for the reaction of dicarbon molecules with $C_2D_2(X^1\Sigma_g^+)$ ($m/z = 50$; C_4D^+; upper left), $^{13}C_2H_2(X^1\Sigma_g^+)$ ($m/z = 51$; $^{13}C_2C_2H^+$; upper right), and $C_2HD(X^1\Sigma^+)$ ($m/z = 50$; C_4D^+; lower left) ($m/z = 49$; C_4H^+; lower right) at a nominal collision energy of 29 kJ mol^{-1}. Circles and 1σ error bars indicate experimental data, and the solid lines, the calculated distributions. CM designates the center-of-mass angle. The corresponding time-of-flight (TOF) spectra are shown in Figure 4.

bond rupture from a tight transition state. We should recall that in the case of indirect, bimolecular reactions involving polyatomic reactants such as reactions of carbon atoms and cyano radicals with unsaturated hydrocarbons, an inherent exit barrier from the fragmenting intermediate to the final reaction products is often accompanied by a $P(E_T)$ peaking away from zero translational energy.[33] From the center-of-mass translational energy distributions, we can compute the averaged translation energy, $\langle E_T \rangle$, and plot the nominal collision energy, E_c, versus the fraction of the energy channeling into the translational modes of the products, $\langle E_r \rangle / E_{max}$. Here, an almost invariant shape is found depicting only a slight increase from about 31 ± 2% to 34 ± 2% from the lowest to the highest collision energy. These data can also be fit with a linear relationship, eq 1.

$$\langle E_T \rangle / E_{Tmax} = (5.5 \pm 0.6) \times 10^{-5} E_c + (0.35 \pm 0.02) \quad (1)$$

As the collision energy increases, the shapes of the $T(\theta)$s and the inherent flux contour maps change (Figures 6 and 7). The distributions vary from a forward scattered distribution with an intensity ratio of $T(\theta)$ at $\theta = 0°$ to 180° of $T(0°)/T(180°) = 2.0 \pm 0.3$ at the lowest collision energy of 10.6 kJ mol^{-1} to a backward scattered distribution with $T(0°)/T(180°) = 0.5 \pm 0.1$ at the highest collision energy of 47.5 kJ mol^{-1}. We would like to comment briefly on angular momentum conservation in this reaction. This system presents a classical example where the incident orbital angular momentum is transformed mainly into the rotational excitation of the linear 1,3-butadienyl radical. The total angular momentum **J** is given by

$$\mathbf{J} = \mathbf{L} + \mathbf{j} = \mathbf{L}' + \mathbf{j}' \quad (2)$$

with the rotational angular momenta of the reactants and products **j** and **j**′ and the initial and final orbital angular momenta **L** and **L**′.[34] Because the reactant beams are prepared in a supersonic expansion, the rotational excitation of the reactant molecules is expected to be small and eq 2 can be simplified:

$$\mathbf{J} \approx \mathbf{L} = \mathbf{L}' + \mathbf{j}' \quad (3)$$

Because kinetic experiments[35] and our electronic structure calculations suggest that the reaction of dicarbon with acetylene

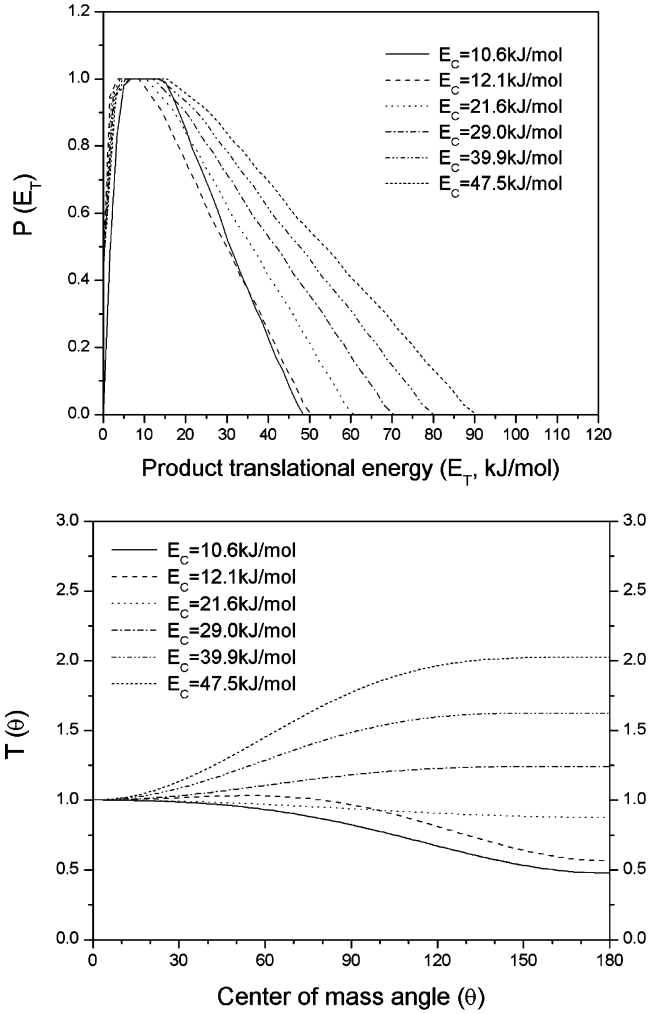

Figure 6. Center-of-mass angular flux distributions (lower) and center-of-mass translational energy flux distributions (upper) for the reaction $C_2(X^1\Sigma_g^+/a^3\Pi_u) + C_2H_2(X^1\Sigma_g^+) \rightarrow C_4H(X^2\Sigma^+) + H(^2S_{1/2})$ at six different collision energies.

has no entrance barrier and proceeds within orbiting limits, the maximum impact parameter b_{max} leading to a complex formation is approximated in terms of the classical capture theory to be between 2.8 Å and 3.8 Å.[36] The maximum orbital angular momentum L_{max} relates to b_{max} via

$$L_{max} = \mu b_{max} v_r \quad (4)$$

where μ is the reduced mass and v_r is the relative velocity of the reactants. This would translate into L_{max} in the range of 90−150 $\hbar$. An upper limit of $\mathbf{L}'$ can also be estimated by assuming a relative velocity of the recoiling products corresponding to the average translational energy release $\langle E_T \rangle$, and choosing an acetylene C≡C-bond length of about 1.1 Å as the exit impact parameter. This calculates L' to be between 20 and 30 $\hbar$ at the collision energies investigated. Therefore, the initial orbital angular momentum is much larger than the final orbital angular momentum; consequently, most of the initial orbital angular momentum channels into rotational excitation of the 1,3-butadienyl radical resulting into relatively weakly polarized $T(\theta)$s. This weak $\mathbf{L}-\mathbf{L}'$ correlation is a direct result of large impact parameters contributing to the complex formation and the inability of the departing hydrogen atom to carry significant orbital angular momentum. Figure 8 summarizes the collision energy dependence of the ratios of the center-of-mass angular distributions at the poles. The data could be fit with eq 5.

$$T(0°)/T(180°) = (0.41 \pm 0.09)(3.53 \pm 0.34)e^{-(E_c/(13.5\pm2.2))} \quad (5)$$

It should be stressed that the TOF spectra (Figure 4) and LAB distributions (Figure 5) of the isotopically labeled reaction products could be fit, within the error limits, with identical center-of-mass translational energies $P(E_T)$ and angular distributions $T(\theta)$ as derived from the C_2/C_2H_2 system at a collision energy of 29 kJ mol^{-1} (Figure 6).

5. Discussion

5.1. Energetical Considerations. We have determined that the formation of the C_4H isomer plus atomic hydrogen is, averaged over six collision energies, exoergic by 39.9 ± 5.0 kJ mol^{-1}. This value is in excellent agreement with the theoretically obtained energy of −41.9 kJ mol^{-1} of the reaction of electronically excited dicarbon in its first excited triplet state, $C_2(a^3\Pi_u)$, with acetylene to form ground-state 1,3-butadiynyl, $C_4H(X^2\Sigma^+)$, plus a hydrogen atom. Note that the energetics of ground-state dicarbon, $C_2(X^1\Sigma_g^+)$, reacting with acetylene are computed to be less favorable by about 7 kJ mol^{-1}; therefore, the experimentally determined energetics of the reactions of ground-state and excited-state dicarbon molecules with acetylene to form ground-state 1,3-butadiynyl plus a hydrogen atom are in line with the computed values. The five C_4H isomers p2−p6 are less stable by 118.0, 140.2, 171.4, 74.8, and 230.6 kJ mol^{-1}, respectively, compared to 1,3-butadiynyl radical (Figure 1). Note that an earlier study of the C_4H isomers suggested another C_{2v} symmetric cyclic isomer, HC═c-C_3, to exist about 165 kJ mol^{-1} above p1.[37] However, we found that HC═c-C_3 actually has one imaginary frequency; once the C_{2v} symmetry is released, it optimizes to p1. Takahashi's study also yielded incorrect ground state of p1 and did not locate p3 and p4 as local minima. Considering the energetics of our calculations (Figure 1), the reaction energies to form p2−p6 are calculated to be +77.6, +99.8, +131.0, +34.4 and +190.2 kJ mol^{-1} on the triplet surface. Because the highest collision energy in our experiment was 47.5 kJ mol^{-1}, these C_4H isomers are energetically not accessible, except p5 at the two highest collision energies. Therefore, we can conclude that the 1,3-butadiynyl radical is the sole C_4H structural isomer formed in the reaction of dicarbon with acetylene on the triplet surfaces at collision energies of 10.6, 12.1, 21.6, and 29.0 kJ mol^{-1}. On the singlet surface, we can exclude p5 at all collision energies except 47.5 kJ mol^{-1}. Because, however, the collision energy dependence of the fraction of the averaged translational energy and of the ratio of the center-of-mass angular distribution at the poles (Figure 8) at both higher collision energies can be fit with the identical functions as at the lower collision energies (eqs 1 and 5), we can likely rule out the involvement of p5 at higher collision energies. Finally, we also compared the computed exoergicities of the reactions of singlet dicarbon with isotopically labeled acetylene reactants (eqs 6−8) with our experimental data of 39.9 ± 5.0 kJ mol^{-1}. Recall that the corresponding reactions with dicarbon in its $a^3\Pi$ state are more exoergic by 7 kJ mol^{-1}. The computed values agree nicely with the experimentally determined energetics; the change of the reaction energies due

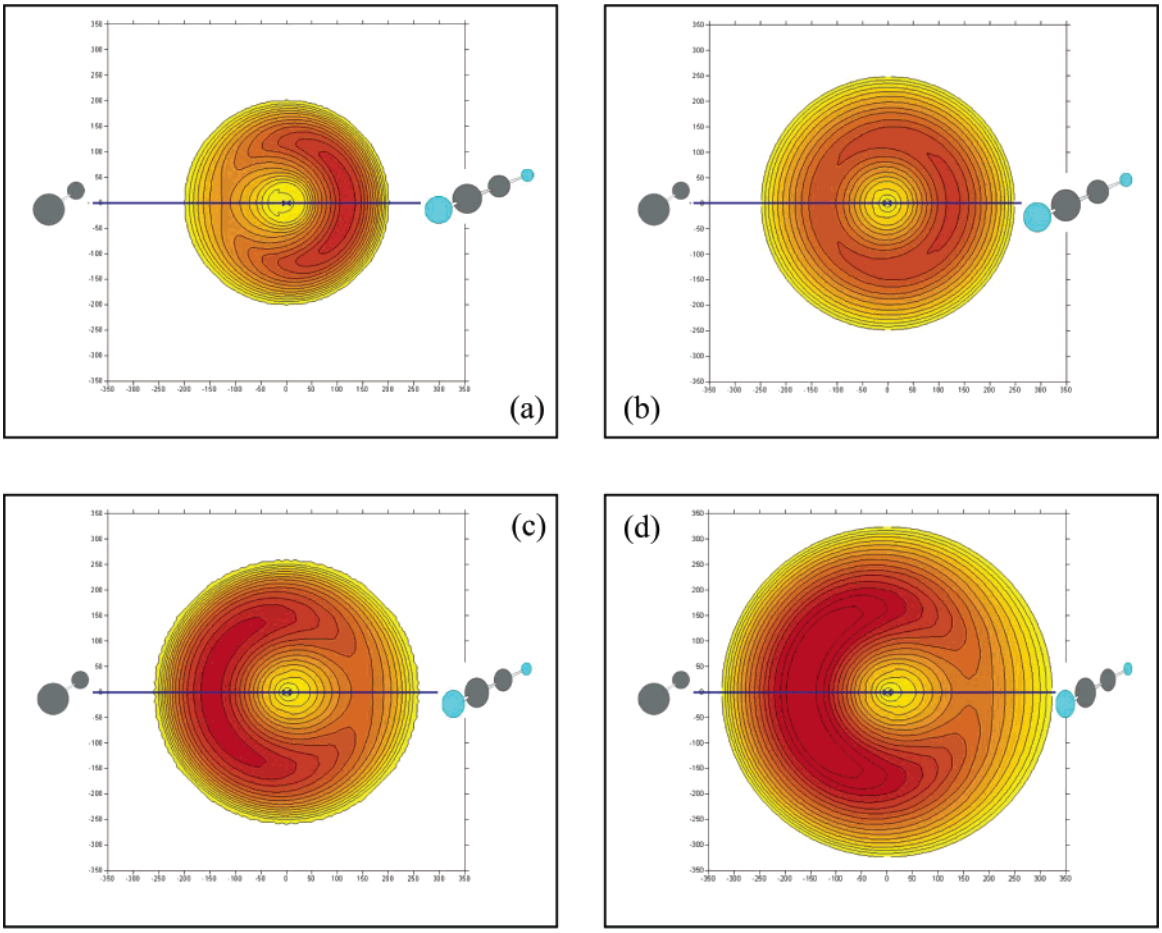

Figure 7. Contour flux maps of the 1,3-butadiynyl radical for the reaction $C_2(X^1\Sigma_g^+/a^3\Pi_u) + C_2H_2(X^1\Sigma_g^+) \rightarrow C_4H\ (X^2\Sigma^+) + H(^2S_{1/2})$ at selected collision energies of 10.6 (a), 21.6 (b), 29.0 (c), and 47.5 kJ mol^{-1} (d). Units of the axes are given in ms^{-1}.

to distinct zero point vibration energies is within the error limits of our measurements.

$$C_2(X^1\Sigma_g^+) + C_2D_2(X^1\Sigma_g^+) \rightarrow C_4D(X^2\Sigma^+) + D(^2S_{1/2}) \qquad \Delta_R G = -26.0\ \text{kJ mol}^{-1} \quad (6)$$

$$C_2(X^1\Sigma_g^+) + {}^{13}C_2H_2(X^1\Sigma_g^+) \rightarrow {}^{13}C_2C_2H(X^2\Sigma^+) + H(^2S_{1/2}) \qquad \Delta_R G = -33.3\ \text{kJ mol}^{-1} \quad (7)$$

$$C_2(X^1\Sigma_g^+) + C_2HD(X^1\Sigma^+) \rightarrow C_4H(X^2\Sigma^+) + D(^2S_{1/2}) \qquad \Delta_R G = -33.4\ \text{kJ mol}^{-1}$$
$$\rightarrow C_4D(X^2\Sigma^+) + H(^2S_{1/2}) \qquad \Delta_R G = -25.9\ \text{kJ mol}^{-1} \quad (8)$$

5.2. Reaction Dynamics. *5.2.1. Singlet Surface.* Having identified the 1,3-butadiynyl radical and its isotopomers as the reaction product of dicarbon with acetylene on the singlet and triplet surfaces, we attempt now to solve the underlying reaction dynamics. A preliminary study of this reaction suggested that, on the singlet surface, the 1,3-butadiynyl radical is synthesized via an indirect reaction mechanism through decomposition of a diacetylene intermediate (s3); the latter was suggested to be formed via an isomerization of the cyclic s2 intermediate. This structure could be accessed from the dicarbon and acetylene reactants either by addition of dicarbon to the carbon−carbon triple bond or via isomerization of s1 (Figure 9).[1] However, this study could not determine if the forward−backward symmetry of this microchannel was the result of a lifetime of the diacetylene intermediate being longer than its rotational period or solely the consequence of the $D_{\infty h}$ symmetry of the "symmetric intermediate" (section 1). Also, the role of the s5 intermediate and its potential role in the molecular hydrogen elimination pathway remained to be resolved.

The isotopic studies of the dicarbon−acetylene-d_1 and dicarbon−acetylene-$^{13}C_2$ reactions at a nominal collision energy of 29 kJ mol^{-1} suggest that the singlet diacetylene intermediate, which resides in a deep potential energy well of 577.1 kJ mol^{-1} with respect to the separated reactants, has a lifetime longer than its rotational period. How can we come to this conclusion? The reaction of singlet dicarbon with acetylene-d_1 eventually leads to a diacetylene-d_1 intermediate. Because one hydrogen atom is replaced by a deuterium atom, the symmetry of this intermediate is reduced to $C_{\infty v}$. In the case of the reaction of singlet dicarbon with acetylene-$^{13}C_2$, the isotopically labeled diacetylene intermediates also belongs to the $C_{\infty v}$ group. Recall that the s2 intermediate undergoes ring opening to diacetylene (s3). According to intrinsic reaction coordinate calculations for the transition state separating s2 and s3, this process is more complicated: one of the carbon atoms of the dicarbon indeed formally inserts between two acetylene carbon atoms, and the second takes the terminal position in the C_4 chain and this is followed by a spontaneous hydrogen shift to this terminal carbon. So, when $C_2(X^1\Sigma_g^+)$ attacks $^{13}C_2H_2(X^1\Sigma_g^+)$, the H^{13}-CC^{13}CCH diacetylene isotopomer is produced after the ring opening process. Therefore, in both the reactions of dicarbon

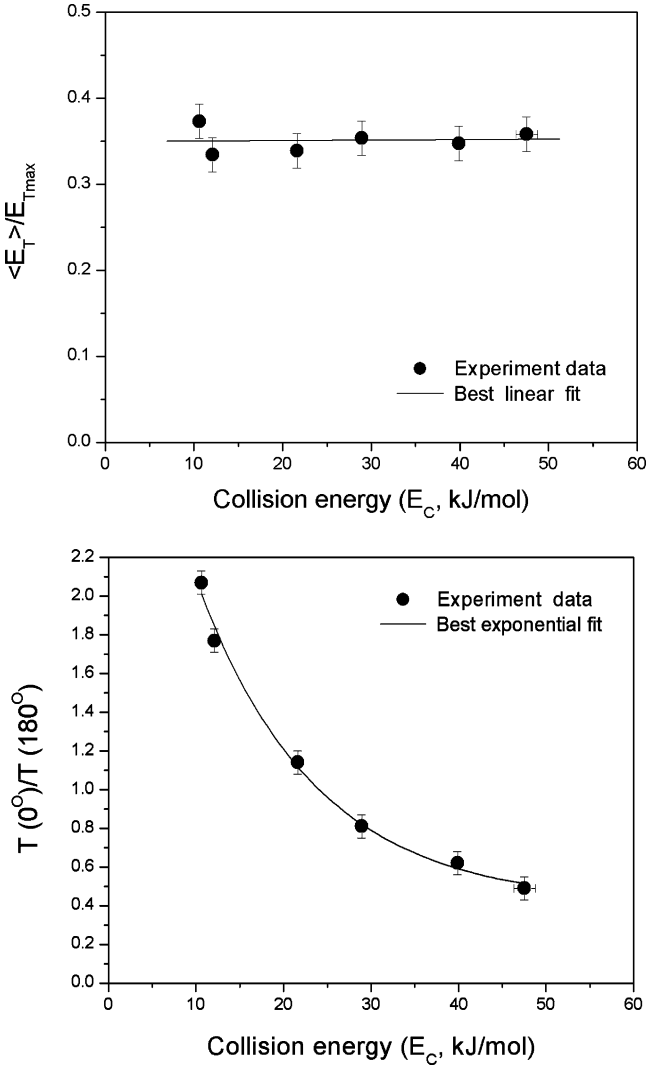

Figure 8. Collision energy dependence of the fraction of the averaged, translational energy of the 1,3-butadiynyl and atomic hydrogen products (upper) and of the intensity ratio of the center-of-mass angular distributions at the poles, $T(0°)/T(180°)$ (lower).

with $C_2HD(X^1\Sigma^+)$ and $^{13}C_2H_2(X^1\Sigma_g^+)$, the symmetry of the diacetylene isotopomer is reduced from $D_{\infty h}$ to $C_{\infty v}$. This eliminates the C_2 rotational axes located perpendicularly to the diacetylene molecular axis. Consequently, both the DCCCCH and $H^{13}CC^{13}CCH$ structures cannot be classified as "symmetric intermediates". Because the TOF data and LAB distributions of the $C_4H(X^2\Sigma^+)$ and $C_4D(X^2\Sigma^+)$ products (decomposition of the DCCCCH intermediate) and $^{13}C_2C_2H(X^2\Sigma^+)$ products (decomposition of the $H^{13}CC^{13}CCH$ intermediate) could be fit with *identical* center-of-mass functions as obtained from the dicarbon−acetylene ($C_2H_2(X^1\Sigma_g^+)$) reaction (section 4), we can deduce that both the symmetry of the diacetylene intermediate ($D_{\infty h}$ versus $C_{\infty v}$) has no effect on the shape of the center-of-mass functions. Therefore, we can conclude that the diacetylene intermediate is long-lived, at least at a collision energy of 29 kJ mol^{-1} as investigated for the isotopically labeled reactants. If the diacetylene isotopomer were short-lived, the center-of-mass angular distributions should have exhibited different shapes compared to the $D_{\infty h}$ symmetric diacetylene molecule. We would like to comment finally on the exit channel of the atomic deuterium/hydrogen loss pathways. The diacetylene molecule can decompose via a loose exit transition state in a barrierless reaction to form $C_4H(X^2\Sigma^+) + H(^2S_{1/2})$ by hydrogen emission within the rotational plane of the complex through a simple bond rupture. The reversed reaction of a hydrogen atom with the 1,3-butadiynyl radical presents a prototype atom-radical recombination reaction without entrance barrier. The loose exit transition state is also reflected in a mild geometry change from the diacetylene intermediate to the 1,3-butadiynyl radical from r(H−C1) = 109.4 pm, r(C1−C2) = 121.8 pm, and r(C2−C3) = 138.3 pm (diacetylene)[38] to r(H−C1) = 106.3 pm, r(C1−C2) = 120.6 pm, r(C2−C3) = 136.5 pm, and r(C3−C4) = 121.1 pm (1,3-butadiynyl). In case of the DCCCCH intermediate, the experiments verify that the diacetylene-d_1 molecule can either lose a hydrogen or deuterium atom via reaction 5. The hydrogen loss from the $H^{13}CC^{13}CCH$ intermediate is actually very interesting. The decomposition of this molecule via atomic hydrogen loss can form two distinct isotopomers of the 1,3-butadiynyl radical, i.e., $H^{13}CC^{13}CC(X^2\Sigma^+)$ and $^{13}CC^{13}CCH$.

It is worth discussing the symmetry of the reactive surface. The $^1\Sigma_g^+$ ground state of the diacetylene molecule correlates with both ground-state $C_4H(X^2\Sigma^+) + H(^2S_{1/2})$ reaction products. As a matter of fact, the point groups of s2 and of the transitions states involved in the s1 → s2 and s2 → s3 rearrangements dictate that C_2 presents the highest feasible symmetry under which this reaction can proceed until the formation of the diacetylene intermediate. However, the 1,3-butadiynyl reaction product belongs to the $C_{\infty v}$ point group and hence loses its C_2 symmetry axis parallel to the principal rotational axis. This reduces the point group and the symmetry of the total electronic wave functions of reactants, involved intermediates, and products to C_1 and ^{1}A, respectively.

Finally, we would like to discuss the potential involvement of two reaction intermediates s4 and s5. A hydrogen migration in s1 could lead to s4; the latter may undergo ring opening to yield butatrienylidenecarbene (s5). On the basis of our calculations, s5 can decompose either via atomic hydrogen loss to form $C_4H(X^2\Sigma^+) + H(^2S_{1/2})$ or through molecular hydrogen loss to yield electronically excited tetracarbon, $C_4(a^1\Sigma_g^+) + H_2(X^1\Sigma_g^+)$ in an endoergic reaction (+ 34.9 kJ mol^{-1}). On the basis of the energetics alone, we could have observed molecular hydrogen at those experiments carried out at collision energies of 39.9 and 47.5 kJ mol^{-1}. However, our data clearly showed no sign of a molecular hydrogen loss, even at an enhanced signal-to-noise ratio of 20−30 compared to an earlier study of this reaction.[1] How can this apparent discrepancy be explained? In principle, the $C_4(a^1\Sigma_g^+) + H_2(X^1\Sigma_g^+)$ products can be formed from the intermediates s3 and s5. However, a careful search of a transition state for molecular hydrogen elimination from diacetylene (s3) showed that no first-order saddle point exists on this pathway. The energies of possible transition-state candidates for such 1,4-H_2 elimination are very high and transition-state optimization converges to the separated $C_4(a^1\Sigma_g^+) + H_2(X^1\Sigma_g^+)$ products. On the other hand, $H_2(X^1\Sigma_g^+)$ loss from s5 takes place without an exit barrier. To prove this, calculations of the minimal energy reaction path (MEP) from $C_4(a^1\Sigma_g^+) + H_2(X^1\Sigma_g^+)$ to s5 were performed by scanning PES keeping the distance from a terminal carbon atom of tetracarbon to the center of the H−H bond frozen at different values from 4.0 to 1.0 Å and optimizing all other geometric parameters. These calculations showed that the energy of the system steadily decreases when $H_2(X^1\Sigma_g^+)$ approaches the terminal carbon atom of $C_4(a^1\Sigma_g^+)$, with a barrierless formation of two new C−H bonds and cleavage of the H−H bond. Thus, just like in the reaction of $CH_2(a^1A_1) + H_2(X^1\Sigma_g^+)$ to form methane, the lone pair of the carbon atom inserts into the H−H bond of molecular hydrogen without a barrier. The s5 → $C_4(a^1\Sigma_g^+) + H_2(X^1\Sigma_g^+)$ reaction step is computed to be highly endothermic, by 429 kJ

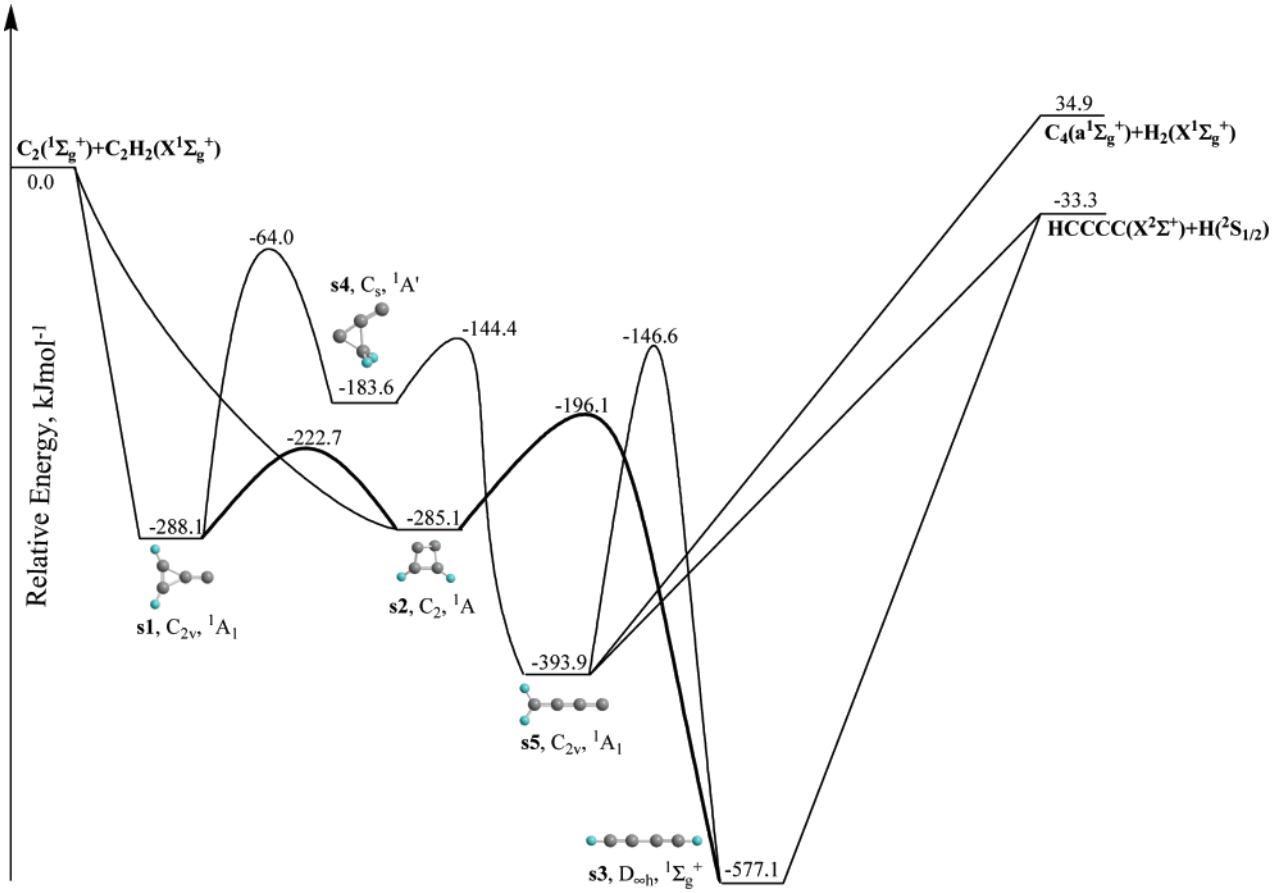

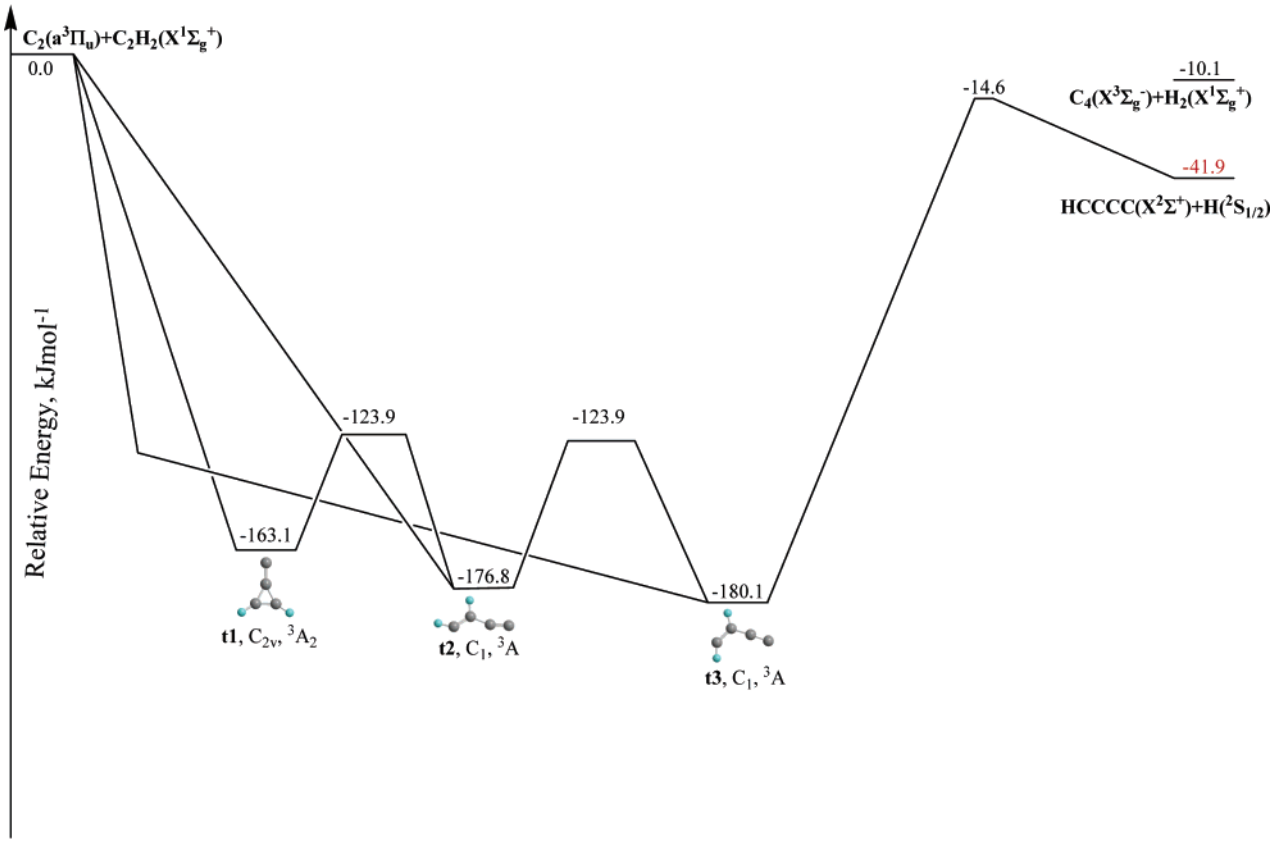

Figure 9. Continued

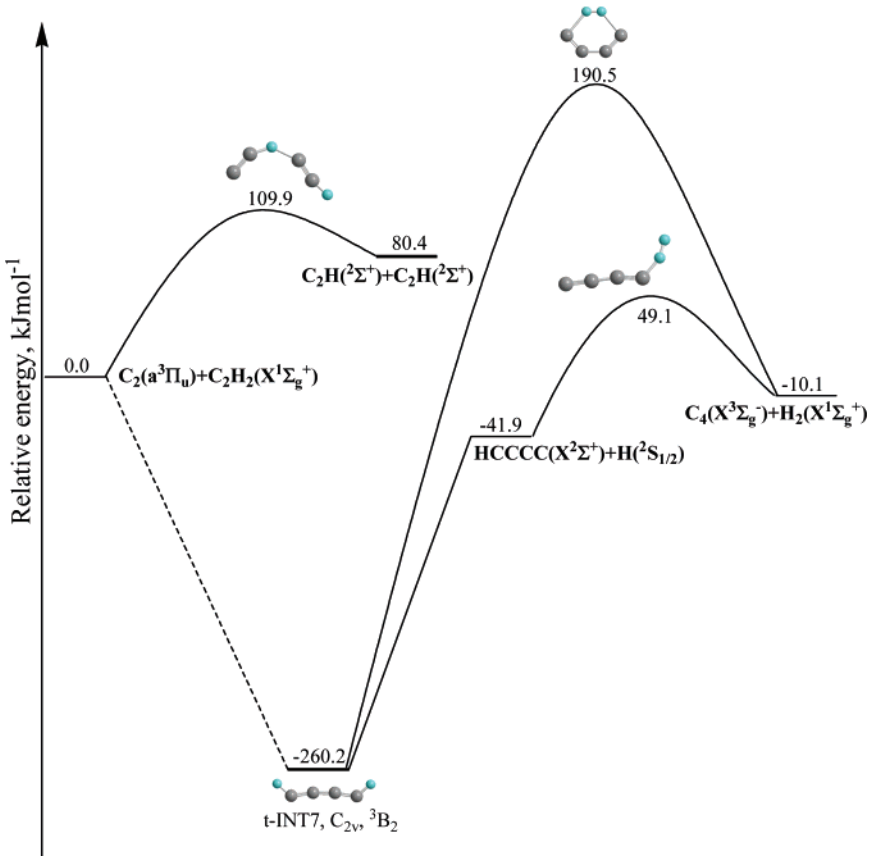

Figure 9. Potential energy surfaces (PES) of the reactions of $C_2(X^1\Sigma_g^+)$ (top) and $C_2(a^3\Pi_u)$ (bottom) with acetylene, $C_2H_2(X^1\Sigma_g^+)$, adapted from ref 1. Reaction pathways to the C_4H isomers p2−p5 (Figure 1) have been omitted (see text for details). The molecular hydrogen elimination and hydrogen abstraction channels on the triplet surface are also included (next page).

mol^{-1}, but it occurs without a distinct transition state and exit barrier. Because we did not observe any molecular hydrogen elimination channel, this suggests that the formation of the s5 intermediate must be hindered. Let us have a closer look at the formation process of s5. Actually, s1 presents the crucial collision complex which can either isomerize to s2 or to s4. Considering the relative barrier heights of 65.4 and 224.1 kJ mol^{-1}, respectively, it is obvious that the s1 → s2 pathway should dominate over the s1 → s4 route. This conclusion is supported by RRKM calculations. The ratio of both rate constants varies from 4.3×10^4 to 4.2×10^3 at collision energies of 0 and 50 kJ mol^{-1}. Thus the channel via s2 is at least 3 orders of magnitude faster than that via s4, and the latter can be safely ruled out. Therefore, both the experiments and electronic structure calculations agree that, at least on the singlet surface, molecular hydrogen should not be formed.

5.2.2. Triplet Surface. We identified the 1,3-butadiynyl radical, $C_4H(X^2\Sigma^+)$, plus a hydrogen atom as the sole reaction products on the triplet surface. What is the actual formation pathway to form the 1,3-butadiynyl radical on the triplet surface? Our previous study suggested that up to three entrance channels could have been involved on the triplet C_4H_2 surface; all pathways have no entrance barrier and proceed via addition of the dicarbon molecule to the carbon−carbon triple bond of the acetylene molecule forming t1, t2, and t3 (Figure 9).[1] However, the relative contribution of these intermediates to the formation of the 1,3-butadiynyl radical product has not been resolved in the earlier study. It should be recalled that the derived center-of-mass angular distributions change from a forward-scattered shape to an enhanced intensity in the backward direction as the collision energy is increased. This asymmetry alone demonstrates that the triplet surface must be involved in the reaction. Recall that on the singlet surface, the "symmetric" diacetylene molecule was identified as the decomposing complex to form the 1,3-butadiynyl molecule. As elucidated in the previous section, the atomic hydrogen emission from the diacetylene molecule always results, due to the symmetry, in a forward−backward symmetric center-of-mass angular distribution. Because s5 was found not to contribute to the formation of the 1,3-butadiynyl radical, there is no intermediate present on the singlet surface that can induce an asymmetry in the center-of-mass angular distributions. Therefore, at least one nonsymmetric intermediate must exist on the triplet surface that can be responsible for a nonsymmetric microchannel on the triplet surface. Among the three initial collision complexes, only t3 can lose a hydrogen atom via a tight transition state located about 26 kJ mol^{-1} above the separated products to form the experimentally observed 1,3-butadiynyl radical plus atomic hydrogen; t1 and t2 have to rearrange to t3 first. The existence of an exit barrier is also reflected in the shape of the center-of-mass translational energy distributions (section 4). Here, a broad distribution maxima of the $P(E_T)$s extending up to 17 kJ mol^{-1} from zero translational energy is evident. Recall that actually the flat plateau accounts for the nature of the exit transitions states in both reaction pathways on the singlet and triplet surfaces: a loose transition state peaking close to zero translation energy (micro channel 1; singlet surface) and a tight transition state depicting a maximum away from zero translational energy (microchannel 2; triplet surface). The latter pathway also correlates nicely with a significant geometry change and hence inherent electron reorganization from the decomposing t3 complex to the 1,3-butadiynyl radical. Here, our computations suggest r(H−C1) = 108.3 pm, r(H−C2) = 108.9 pm, r(C1−C2) = 135.1 pm, r(C2−C3) = 138.8 pm, and

r(C3−C4) = 127.9 pm (t3) compared to r(H−C1) = 106.3 pm, r(C1−C2) = 120.6 pm, r(C2−C3) = 136.5 pm, and r(C3−C4) = 121.1 pm (1,3-butadiynyl). Note that although the reversed reaction between 1,3-butadiynyl and atomic hydrogen presents formally an atom−radical reaction, this reaction does not portray a simple recombination of two radical centers as found on the singlet surface, but rather an addition of the hydrogen atom to a carbon−carbon triple bond of the 1,3-butadiynyl radical. We can compare the order of magnitude of the barrier to addition as found experimentally (about 17 kJ mol^{-1}) and computationally (26 kJ mol^{-1}) with a related system, i.e., the addition of atomic hydrogen to the carbon−carbon triple bond of acetylene, $C_2H_2(X^1\Sigma_g^+)$.[39] Here, the barrier of 19.7 kJ mol^{-1} compares favorably well with the 1,3-butadiynyl plus atomic hydrogen reaction.

Having identified the feasible collision complexes (t1, t2, and t3) and also the fragmenting intermediate to form the 1,3-butadiynyl radical plus atomic hydrogen, we discuss now two possibilities how the switch from an enhanced intensity in the forward to the backward direction with respect to the dicarbon beam can be explained.[40] First, the change in shape could be rationalized with a change of reactive impact parameter in a similar way as found, for instance, in the crossed beams reactions of atomic carbon with benzene[41] and 1,2-butadiene.[42] Because the reaction has no entrance barrier, we would expect that the maximum impact parameter leading to reaction drops as the collision energy is being increased. In other words, at low collision energies, large impact parameters should dominate. On the basis of the geometry of t1, t2, and t3, both latter structures should be favorably formed from dicarbon molecules holding large impact parameters (low collision energies). This would lead to a forward-scattered distribution of the 1,3-butadiynyl radical with respect to the dicarbon beam. On the other hand, small impact parameters at higher collision energies are expected to yield predominantly t1; in the limiting case, the dicarbon molecule would collide with zero impact parameter under C_{2v} symmetry with the center-of-mass of the acetylene molecule; this would be reflected in a backward scattering of the 1,3-butadiynyl radical with respect to the dicarbon beam. In this scenario, the experimentally found switch from a forward to backward scattered flux contour maps can be reasonably understood in terms of an impact-parameter dictated reaction dynamics of barrierless entrance channels, i.e., an initial formation of t2 and t3 at lower collision energies and inherent larger impact parameters and a preferential collision complex t1 as the collision rises and the maximum impact parameter decreases. Second, we should recall that we have currently no means to quantify the concentration of dicarbon molecules in its triplet state. Therefore, the shape in the center-of-mass angular distribution may also correlate with an increase in concentration of triplet dicarbon as the collision energy increases. Recall that in supersonic beams generated via laser ablation sources, the faster the selected part of the beam is, the higher the concentration of, for instance, vibrationally excited cyano radicals[43] and electronically excited carbon[44] atoms is. In the future it is certainly desirable to quantify the concentration of singlet versus triplet dicarbon to address this issue. Nevertheless, as stated in the previous sections, the asymmetry of the center-of-mass angular distributions can only be rationalized if the triplet surface is involved in the reaction. Could intersystem crossing (ISC) from the triplet to the singlet surface be effective? Recall that the TOF and LAB distributions of the C_2/C_2D_2 and $C_2/^{13}C_2H_2$ systems could be fit with identical center-of-mass functions as for the C_2/C_2H_2 reaction. Therefore, although the mass of the reactant molecules is increased by 2 amu and hence ISC should be facilitated, we have no evidence that, at least at the collision energy investigated, ISC is effective.

TABLE 2: Reaction Enthalpies of Exit Channels of the $C_2(X^1\Sigma_g^+) + C_2H_2(X^1\Sigma_g^+)$ Reaction

	products	reaction enthalpy, kJ mol^{-1}
1	$C_4H(X^2\Sigma^+) + H(^2S_{1/2})$	−33
2	$C_4(X^3\Pi_u) + H_2(X^1\Sigma_g^+)$	−2
3	$c\text{-}C_3H_2(X^1A_1) + C(^3P_j)$	+152
4	$c\text{-}C_3H(X^2B_1) + CH(X^2\Pi)$	+246
5	$CH_2(X^3B_1) + C_3(X^1\Sigma_g^+)$	+142
6	$C_2H(X^2\Sigma^+) + C_2H(X^2\Sigma^+)$	+89

We would like to stress that although the reaction on the singlet and on the triplet surface yield the 1,3-butadiynyl radical, the rovibrational excitation on both surfaces is expected to differ significantly. Recall that in the crossed beam reaction of singlet dicarbon with $^{13}C_2H_2(X^1\Sigma_g^+)$, this reaction would yield distinct $H^{13}CC^{13}CC(X^2\Sigma^+)$ and $HC^{13}CC^{13}C(X^2\Sigma^+)$ isotopomers, as discussed in section 5.2.1. However, on the triplet surface, dicarbon is found to be connected "end on" to only one acetylene carbon atom the decomposing intermediate t3. This will provide solely the $HCC^{13}C^{13}C(X^2\Sigma^+)$ isotopomer on the triplet surface.

Finally, it is important to discuss the possibility of eliminating molecular hydrogen on the triplet surface. Here, the $C_4(X^3\Sigma_g^-) + H_2(X^1\Sigma_g^+)$ products lie 10.1 kJ mol^{-1} below the reactants; the potential precursors for molecular hydrogen elimination is a hitherto not discussed HCCCCH (t-INT7). This transition state has a six-member ring structure and lies very high in energy, 190.5 kJ mol^{-1} above $C_2(a^3\Pi_u) + C_2H_2(X^1\Sigma_g^+)$ (Figure 9). Thus, the forward and reverse barriers for H_2 ($X^1\Sigma_g^+$) elimination from t7 are 450.7 and 200.6 kJ mol^{-1}, and this channel is very unfavorable. This correlates nicely with the failed detection of molecular hydrogen in the crossed beams experiments. If we consider the reverse reaction of $C_4(X^3\Sigma_g^-)$ with $H_2(X^1\Sigma_g^+)$, tetracarbon can be looked at as a σ-radical, similar to $C_2H_3(X^2A')$, $C_2H(X^2\Sigma^+)$, or $HCCCC(X^2\Sigma^+)$. We have demonstrated earlier,[45] on the basis of the molecular orbital consideration, that $H_2(X^1\Sigma_g^+)$ addition to such σ-radical is not possible; all of them prefer to react with molecular hydrogen by hydrogen abstraction. This also makes the reverse reactions of molecular hydrogen elimination unlikely because an atomic hydrogen loss followed by a hydrogen abstraction is more favorable.

5.3. Undetected Channels. Table 2 compiles the energetics of alternative exit channels. It is evident that the competing exit channels (3)−(6) are too endoergic to be relevant even at the highest collision energy of 47.5 kJ mol^{-1} as employed in the present study. On the basis of the energetics, the formation of two ethynyl radicals (channel (6)) might show minor contribution in the high energy tail of the Maxwell−Boltzmann distribution in high-temperature flames (5000 K). In the triplet electronic state, dicarbon can also react with acetylene via hydrogen abstraction through direct scattering dynamics producing $C_2H(X^2\Sigma^+) + C_2H(X^2\Sigma^+)$. Considering the reaction of triplet dicarbon with $^{13}C_2H_2$ ($X^1\Sigma_g^+$), we expect to form only CCH-($X^2\Sigma^+$) + $^{13}C^{13}CH(X^2\Sigma^+)$. The barrier for this abstraction process is calculated to be rather high, 109.9 kJ mol^{-1}. However, a direct hydrogen abstraction is not possible in the ground singlet state. Here, the $C_2(X^1\Sigma_g^+)$ addition to the acetylene molecule is a much more favorable process. The abstraction pathway in the singlet state might be possible if we consider an excited open-shell singlet surface. Using a transition-state search for the open-shell singlet $^1A''$ state, we were able to locate a stationary point corresponding to the hydrogen abstraction process. However, this structure has two imaginary frequencies

and lies about 25 kJ mol^{-1} higher in energy (at the B3LYP level without zero point energy) than the hydrogen abstraction transition state in the triplet state and correlates to the excited state of the $C_2H(X^2\Sigma^+) + C_2H(A^2\Pi)$ products. We can conclude here that the direct hydrogen abstraction process to form ethynyl radicals is not possible under present experimental conditions on the singlet surface. Nevertheless, we identified the diacetylene molecule (s3) as the decomposing intermediate to form 1,3-butadiynyl plus atomic hydrogen. On the other hand, diacetylene could undergo a carbon−carbon single bond rupture producing $C_2H(X^2\Sigma^+) + C_2H(X^2\Sigma^+)$. In this scenario, the formation of the ethynyl radical presents proceeds through indirect scattering dynamics; in a reaction of singlet dicarbon with $^{13}C_2H_2(X^1\Sigma_g^+)$, we would expect solely $C^{13}CH\ (X^2\Sigma^+) + {}^{13}CCH(X^2\Sigma^+)$ to be synthesized. Nevertheless, the overall energetics should favor the hydrogen elimination pathway from s3 compared to the carbon−carbon bond rupture process. As a matter of fact, in our crossed beams experiments, reaction 6 is too endoergic to proceed.

6. Conclusions

We investigated the reaction of dicarbon molecules in their electronic ground, $C_2(X^1\Sigma_g^+)$, and first excited state, $C_2(a^3\Pi_u)$, with acetylene, $C_2H_2(X^1\Sigma_g^+)$, to form the 1,3-butadiynyl radical, $C_4H(X^2\Sigma^+)$, plus a hydrogen atom under single collision conditions at six different collision energies between 10.6 and 47.5 kJ mol^{-1}. These studies were augmented by crossed molecular beam experiments of dicarbon with three isotopomers $C_2D_2(X^1\Sigma_g^+)$, $C_2HD(X^1\Sigma^+)$, and $^{13}C_2H_2\ (X^1\Sigma_g^+)$ to elucidate a potential intersystem crossing (ISC) and the effect of the symmetry of the reaction intermediate(s) on the center-of-mass angular distributions. On the singlet surface, dicarbon was found to react with acetylene without entrance barrier through an indirect reaction mechanism involving a diacetylene intermediate. The latter decomposed via a loose exit transition state by an emission of a hydrogen atom to form the 1,3-butadiynyl radical $C_4H(X^2\Sigma^+)$; the overall reaction was found to be exoergic by about 33 kJ mol^{-1}. The $D_{\infty h}$ symmetry of the decomposing diacetylene intermediate results in collision-energy invariant, isotropic (flat) center-of-mass angular distributions of this microchannel. Isotopic substitution experiments suggested that at least at a collision energy of 29 kJ mol^{-1}, the diacetylene isotopomers are long-lived with respect to their rotational periods. On the triplet surface, the reaction involved three feasible addition complexes t1, t2, and t3. All three initial collision complexes are located in shallower potential energy wells as compared to diacetylene on the singlet surface, which could lead to a lifetime shorter than the rotation period of these intermediates. The involvement of the triplet surface accounted for the asymmetry of the center-of-mass angular distributions. On both the singlet and triplet surface, neither intersystem crossing nor a molecular hydrogen elimination pathway was found to play a role. The explicit identification of the 1,3-butadiynyl radical, $C_4H(X^2\Sigma^+)$, in the crossed beam reaction of dicarbon molecules with acetylene presents compelling evidence that the 1,3-butadiynyl radical can be formed via bimolecular reactions involving carbon clusters in circumstellar envelopes of dying carbon stars and also in combustion flames.

Acknowledgment. The experimental and theoretical work was supported by the US Department of Energy-Basic Energy Sciences (DE-FG02-03ER15411 (UH) and DE-FG02-04ER15570 (FIU)); the construction of the crossed beams machine was also aided by the National Science Foundation (CHE-0234461).

References and Notes

(1) Kaiser, R. I.; Balucani, N.; Charkin, D. O.; Mebel, A. M. *Chem. Phys. Lett.* **2003**, *382*, 112.

(2) Heath, J. R. In *Fullerenes*; Hammond, G. S., Kuck, V. J., Eds.; American Chemical Society: Washington, DC, 1992.

(3) Minh, Y. C.; van Dishoeck, E. F. *Astrochemistry: From Molecular Clouds to Planetary Systems*; Astronomical Society of the Pacific: San Francisco, 2000.

(4) Millar, T. J.; Farquhar, P. R. A.; Willacy, K. *Astron. Astrophys. Suppl. Ser.* **1997**, *121*, 139.

(5) Doty, S. D.; Leung, C. M. *Astrophys. J.* **1998**, *502*, 898.

(6) Chemistry and Physics of Molecules and Grains in Space. *Faraday Discuss.* **1998**, *109*.

(7) Sykes, M. V. *The Future of Solar System Exploration*; Astronomical Society of the Pacific: San Francisco, 2002.

(8) Summers, M. E.; Strobel, D. F. *Astrophys. J.* **1989**, *346*, 495.

(9) Kiefer, J. H.; Sidhu, S. S.; Kern, R. D.; Xie, K.; Chen, H.; Harding, L. B. *Combust. Sci. Technol.* **1992**, *82*, 101.

(10) Hausmann, M.; Homann, K. H. 22nd International Annual Conference of ICT. *Combust. React. Kinet.* **1991**, 1.

(11) Zhang, H. Y.; McKinnon, J. T. *Combust. Sci. Technol.* **1995**, *107*, 261.

(12) Dismuke, K. I.; Graham, W. R. M.; Weltner, W., Jr. *J. Mol. Spectrosc.* **1975**, *57*, 127.

(13) Gottlieb, C. A.; Gottlieb, E. W.; Thaddeus, P.; Kawamura, H. *Astrophys. J.* **1983**, *275*, 916.

(14) Yamamoto, S.; Saito, S.; Guelin, M.; Cernicharo, J.; Suzuki, H.; Ohishi, M. *Astrophys. J.* **1987**, *323*, L149.

(15) McCarthy, M. C.; Gottlieb, C. A.; Thaddeus, P.; Horn, M.; Botschwina, P. *J. Chem. Phys.* **1995**, *103*, 7820.

(16) Chen, W.; Novick, S. E.; McCarthy, M. C.; Gottlieb, C. A.; Thaddeus, P. *J. Chem. Phys.* **1995**, *103*, 7828.

(17) Wing, R. F. *The Carbon Star Phenomenon*; International Astronomical Union, Kluwer: Dordrecht, The Netherlands, 2000.

(18) Guelin, M.; Green, S.; Thaddeus, P. *Astrophys. J.* **1978**, *224*, L27.

(19) Cernicharo, J.; Goicoechea, J. R.; Benilan, Y. *Astrophys. J.* **2002**, *580*, L157.

(20) Nejad, L. A. M.; Millar, T. J. *A&A* **1987**, *183*, 279.

(21) Kaiser, R. I.; Mebel, A. M.; Balucani, N.; Lee, Y. T.; Stahl, F.; Schleyer, P. v. R.; Schaefer, H. F. *Faraday Discuss.* **2001**, *119*, 51.

(22) Kaiser, R. I.; Ochsenfeld, C.; Head-Gordon, M.; Lee, Y. T.; Suits, A. G. *Science* **1996**, 274, 1508.

(23) Guo, Y.; Gu, X.; Kaiser, R. I. *Int. J. Mass. Spectrom.* **2006**, *249*−*250*, 420. Gu, X.; Guo, Y. Kaiser, R. I. *Int. J. Mass. Spectrom.* **2005**, *246*, 29. Gu, X.; Guo, Y.; Kawamura, E.; Kaiser, R. I. *Rev. Sci. Instrum.* **2005**, *76* 083115. Guo, Y.; Gu, X.; Kawamura, E.; Kaiser, R. I. *Rev. Sci. Instrum.* **2006**, *77*, 034701.

(24) Gu, X.; Guo, Y.; Kawamura, E.; Kaiser, R. I. *J. Vac. Sci. Technol. A* **2006**, *24*, 505.

(25) Gu, X.; Guo, Y.; Kaiser, R. I. *J. Phys. Chem. A* **2006**, submitted.

(26) Kaiser, R. I.; Lee, Y. T.; Suits, A. G. *J. Chem. Phys.* **1995**, *103*, 10395.

(27) Weis, M. S. Ph.D. Thesis, University of California, Berkeley, 1986.

(28) Vernon, M. Thesis, University of California, Berkeley, 1981.

(29) Becke, A. D. *J. Chem. Phys.* **1993**, *98*, 5648. Lee, C.; Yang; W.; Parr, R. G. *Phys. Rev. B* **1988**, *37*, 785.

(30) Purvis, G. D.; Bartlett, R. J. *J. Chem. Phys.* **1982**, *76*, 1910.

(31) Frisch, M. J.; Trucks, G. W.; Schlegel, H. B.; Scuseria, G. E.; Robb, M. A.; Cheeseman, J. R.; Zakrzewski, V. G.; Montgomery, J. A., Jr.; Stratmann, R. E.; Burant, J. C.; Dapprich, S.; Millam, J. M.; Daniels, A. D.; Kudin, K. N.; Strain, M. C.; Farkas, O.; Tomasi, J.; Barone, V.; Cossi, M.; Cammi, R.; Mennucci, B.; Pomelli, C.; Adamo, C.; Clifford, S.; Ochterski, J.; Petersson, G. A.; Ayala, P. Y.; Cui, Q.; Morokuma, K.; Malick, D. K.; Rabuck, A. D.; Raghavachari, K.; Foresman, J. B.; Cioslowski, J.; Ortiz, J. V.; Stefanov, B. B.; Liu, G.; Liashenko, A.; Piskorz, P.; Komaromi, I.; Gomperts, R.; Martin, R. L.; Fox, D. J.; Keith, T.; Al-Laham, M. A.; Peng, C. Y.; Nanayakkara, A.; Gonzalez, C.; Challacombe, M.; Gill, P. M. W.; Johnson, B. G.; Chen, W.; Wong, M. W.; Andres, J. L.; Head-Gordon, M.; Replogle, E. S.; Pople, J. A. *GAUSSIAN 98*, revision A.7.; Gaussian Inc.: Pittsburgh, PA 1998.

(32) MOLPRO is a package of ab initio programs written by H. J. Werner and P. J. Knowles, with contributions from J. Almlóf et al.

(33) Kaiser, R. I.; Mebel, A. M. *Int. Rev. Phys. Chem.* **2002**, *21*, 307. Kaiser, R. I.; Balucani, N. *Acc. Chem. Res.*, **2001**, *34*, 699.

(34) Miller, W. B.; Safron, S. A.; Herschbach, D. R. *Discuss. Faraday Soc.* **1967**, *44*, 108.

(35) Smith, I. W. M.; Sage, A. M.; Donahue, N. M.; Herbst, E.; Quan, D. *Faraday Discuss.* **2006**, DOI: 10.1039/b600721j.

(36) Kaiser, R. I.; Lee, Y. T.; Suits, A. G. *J. Chem. Phys.* **1996**, *105*, 8705. Levine, R. D. *Molecular Reaction Dynamics*; Cambridge, U.K., 2005.

(37) Takahashi, J. *Publ. Astron. Soc. Jpn.* **2000**, *52*, 401.

(38) Tanimoto, M.; Kuchitsu, K.; Morino, Y. *Bull. Chem. Soc. Jpn.* **1969**, *42*, 2519.

(39) Zhang, P.; Irle, S.; Morokuma, K.; Tschumper, G. S. *J. Chem. Phys.* **2003**, *119*, 6524.

(40) It should be outlined that the center-of-mass angular distribution at a collision energy of 24.1 kJ mol^{-1} obtained from our earlier study of this reaction (ref 1) differs from the present study. Because both data sets were recorded with different ablation source geometries, distinct laser powers, and parts of the pulsed ablation beam, it is likely that the dicarbon beams in both studies have different ratios of singlet versus triplet dicarbon. This may effect the relative contribution of the scattering signal to the micro channels originating from the singlet and triplet surfaces.

(41) Bettinger, H. F.; Schleyer, P. v. R.; Schreiner, P. R.; Schaefer, H. F., III; Kaiser, R. I.; Lee, Y. T. *J. Chem. Phys.* **2000**, *113*, 4250.

(42) Balucani, N.; Lee, H. Y.; Mebel, A.; Lee, Y. T.; Kaiser, R. I. *J. Chem. Phys.* **2001**, *115*, 5107.

(43) Kaiser, R. I.; Ting, J. W.; Huang, L. C. L.; Balucani, N.; Asvany, O.; Lee, Y. T.; Chan, H.; Stranges, D.; Gee, D. *Rev. Sci. Instrum.* **1999,** *70*, 4185.

(44) Kaiser, R. I.; Mebel, A.; Lee, Y. T. *J. Chem. Phys.* **2001**, *114*, 231.

(45) Kim, G.-S.; Nguyen, T. L.; Mebel, A. M.; Lin, S. H.; Nguyen, M. T. *J. Phys. Chem. A* **2003**, *107*, 1788. Mebel, A. M.; Morokuma, K.; Lin, M. C. *J. Chem. Phys.* **1995**, *103*, 3440. Kurosaki, Y.; Takayanagi, T. *J. Chem. Phys*. **2000**, *113*, 4060. Le, T. N.; Mebel, A. M.; Kaiser, R. I. *J. Comput. Chem.* **2001**, *22*, 1522.